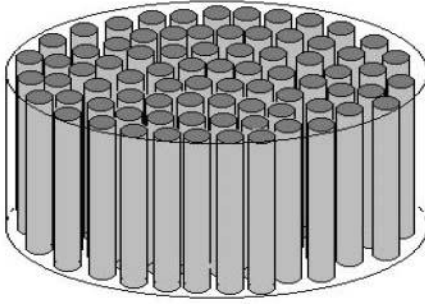


Electroceramic fibres and composites for intelligent apparel applications

HELEN LAI-WA CHAN,
KUN LI and CHUNG LOONG CHOY
The Hong Kong Polytechnic University, Hong Kong

3.1 Introduction

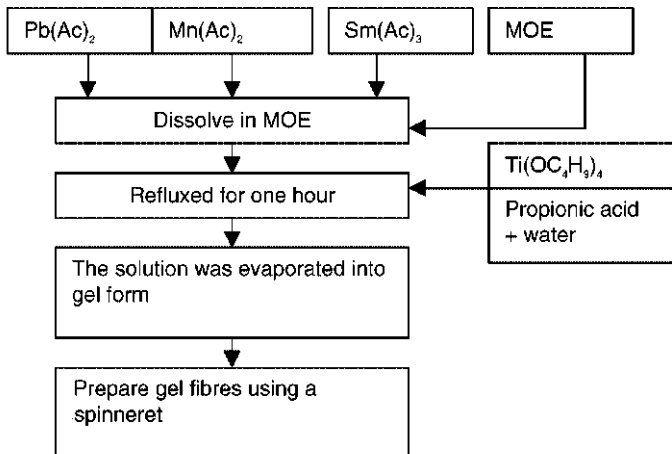
Piezoelectric ceramics are smart materials commonly used in mechatronic devices and smart systems.¹⁻⁵ They can be used to sense changes in pressure and strain in the environment and can generate electrical responses. These electrical signals can be input to feedback systems to stimulate movements in actuators, to trigger alarms or to switch the systems on or off. They are widely used in devices such as accelerometers, microphones and ultrasonic transducers to detect vibrations, acoustic waves and ultrasound. These electroactive ceramics can be fabricated into fibre form using either the viscous suspension spinning process (VSSP) or by the sol-gel process.⁶⁻²⁴ Sol-gel lead zirconate titanate (PZT) fibres have been incorporated into carbon fibre/polymer composites¹³⁻¹⁵ to be used as sensors and actuators in smart structures for aerospace applications. To overcome the brittleness of ceramic fibres and to increase the versatility of their applications, ceramic fibres are often incorporated into polymer matrices to form 1-3 composites.^{7, 10, 11, 17-24} Figure 3.1 shows a schematic diagram of a 1-3 ceramic fibre/polymer composite consisting of one-dimensionally connected ceramic fibres embedded in a three-dimensionally connected polymer matrix.^{19, 25} The advantages of 1-3 composites are that, compared to piezoceramics, they have a lower acoustic impedance ($Z_a = \text{density} \times \text{velocity}$), which is closer to the acoustic impedance of water and human tissues. Hence, when used in medical ultrasound and underwater acoustics, 1-3 piezoelectric ceramic/polymer composites can enhance the efficiency of energy coupling. In addition, they can decouple the thickness mode from the lateral modes and enable the input energy to propagate in the direction of thickness.²⁵⁻⁴⁶ In this chapter, the fabrication of samarium and manganese doped lead titanate ($\text{Pb}_{0.85}\text{Sm}_{0.1}\text{Ti}_{0.98}\text{Mn}_{0.02}\text{O}_3$, PSmT) ceramic fibres by a sol-gel process is described. The fabrication, characterisation and theoretical modelling of ceramic fibre/polymer 1-3 composites are given. Possible ways of using these electroceramic fibres and composites in intelligent apparel applications are also suggested.



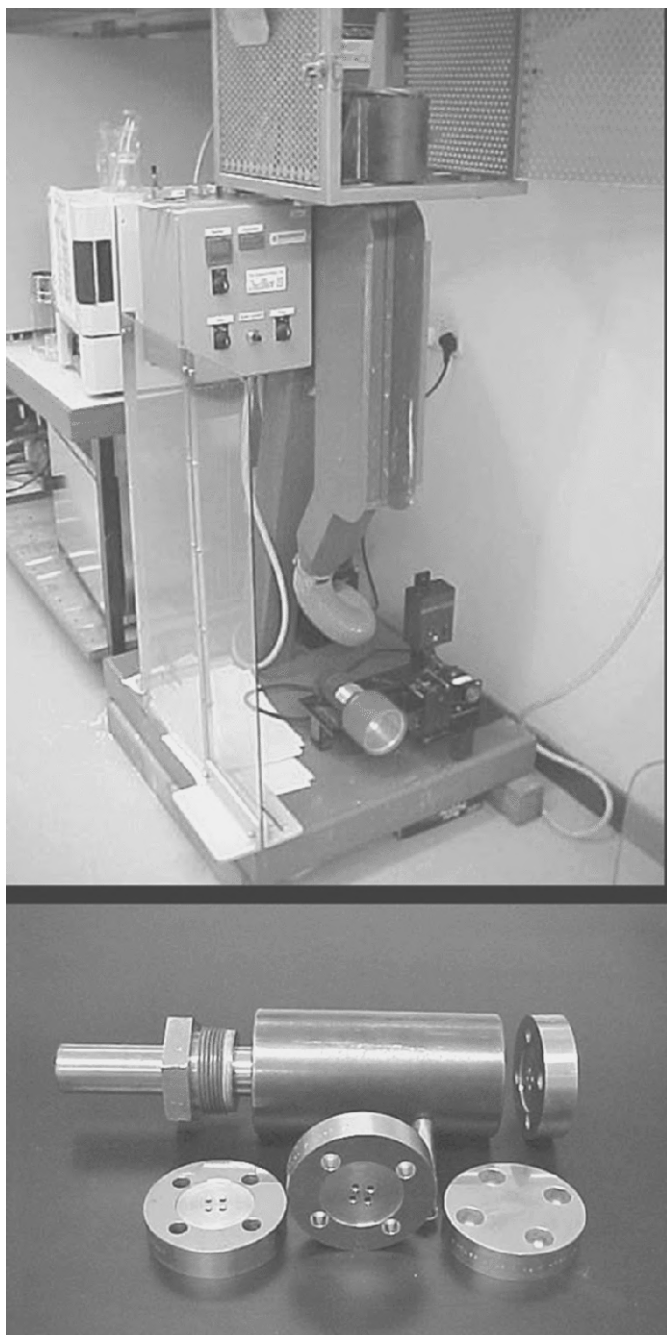
3.1 Schematic diagram of a ceramic fibre/polymer 1-3 composite.¹⁹

3.2 Fabrication of samarium and manganese doped lead titanate fibres

Lead zirconate titanate (PZT) and lead titanate (PT) are electroceramics widely used in transducer and sensor applications as they can be doped with various dopants to modify their properties. The fabrication of PZT fibres has been described in previous reports.^{8, 10, 11, 15, 16, 17, 21, 23} In this work, the fabrication of samarium and manganese doped lead titanate ($\text{Pb}_{0.85}\text{Sm}_{0.1}\text{Ti}_{0.98}\text{Mn}_{0.02}\text{O}_3$, PSmT) by a sol-gel process^{19,20,22,24} is described. PSmT is a piezoelectric ceramic with large anisotropy. It has a high thickness electromechanical coupling coefficient k_t and a low planar electromechanical coupling coefficient k_p . Its $k_t:k_p$ ratio is about 10:1 and it has a low relative permittivity (~ 180). In other words, when a PSmT ceramic disk vibrates in the thickness (z) direction, it has a minimal Poisson's ratio effect



3.2 Block diagram showing the preparation of PSmT gel fibres.¹⁹



3.3 The fibre spinning machine (OneShot III from Alex James & Assoc., Inc, USA) and the spinnerets.¹⁹



3.4 Photograph of PSmT gel fibres.¹⁹

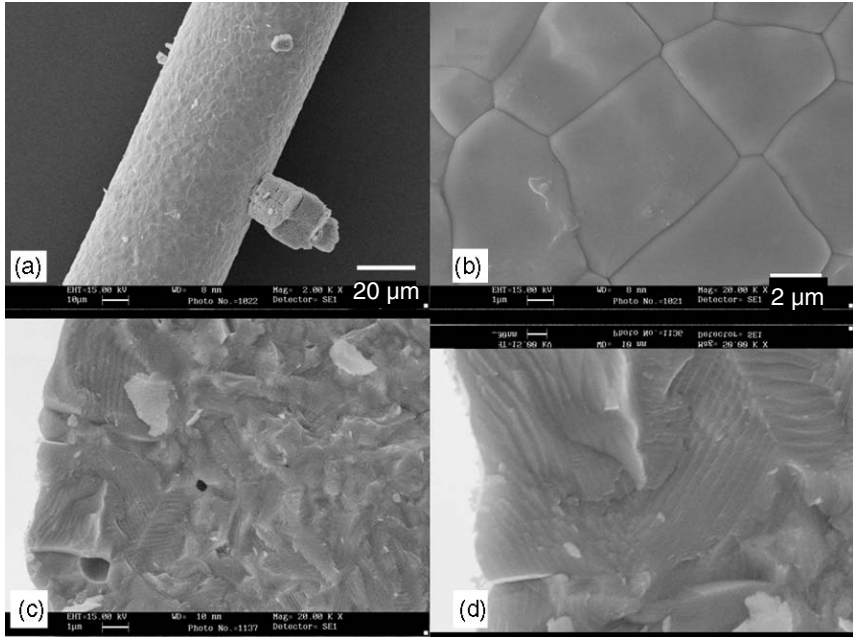
and will only induce negligible vibrations in the planar (x and y) directions. Hence, nearly all of the input energy can be delivered in the thickness direction.

In the sol–gel process, as shown schematically in Fig. 3.2, lead acetate trihydrate (with 2% Pb excess), manganese acetate dihydrate and samarium acetate hydrate were heated at 135°C for 8 h to remove the water of hydration, and then dissolved in methoxyethanol (MOE). Titanium n-butoxide was added to the solution and stirred for 30 min to form a samarium and manganese modified lead titanate solution. The solution was then filtered and concentrated. A mixture of water, methoxyethanol and propionic acid (in a molar ratio of 1:5:3) was added. The solution was refluxed for 30 min at 124°C and then evaporated until a gel-like texture had been attained. The gel was poured into the sample chamber of a Model III spinning apparatus manufactured by Alex James and Associates, Greenville, USA. It was extruded into fibre through the die or spinneret (Fig. 3.3) with a 100 μm diameter pinhole (the size of the pinhole can be varied to produce fibres of different diameters) at $\sim 70^\circ\text{C}$. The fibre was then collected on a spindle. Figure 3.4 shows a bunch of PSmT gel fibres. The gel fibres were tied together, dried and hydrolysed at room temperature for more than a week before being dried at 60–80°C for 48 h. To allow the organic components inside the fibres to escape in a controlled way, the fibres were placed on top of a layer of ceramic powder with the same composition as the fibres. A spoonful of carbon black was scattered around the fibre bundle to reduce the oxygen pressure during heating. The whole setup was then covered with a crucible to pyrolyse at 400°C for 1 h and at 550°C for 1 h. The pyrolysed fibres were calcinated at 850°C for more than 2 h to achieve a complete reaction of the oxides to form PSmT and to densify the fibres.

After calcination at 850°C, the fibres were sintered at 1150°C for 1.5 h. Figure 3.5 (a) to (d) shows the scanning electron micrographs (using a SEM Leica Stereo Scan 440) of the surfaces and the cross sections of a PSmT ceramic fibre. It can be seen that the PSmT fibre is relatively dense without many pores and the average grain size is $\sim 6 \mu\text{m}$. The X-ray diffraction (XRD) patterns (Fig. 3.6) measured using an X-ray diffractometer (Philips X'pert PW 3710) show how the crystalline phases of the PSmT ceramics evolved with different heat-treatment temperatures. It can be seen that the PSmT ceramic fibre that was annealed at 750°C for 1 h has started to form a tetragonal structure. When sintered at 1150°C, it has a tetragonal crystal structure with $c/a \sim 1.0439$ (where a and c are the axes of the tetragonal unit cell), which is comparable to that of the bulk PSmT ceramics.

3.3 Fabrication of ceramic fibre/epoxy 1-3 composites

A bundle of the sintered ceramic fibres was inserted into a plastic tube with its axis aligned parallel to the tube axis. The tube was then filled with epoxy (e.g. Spurr epoxy, hardness B, Emersion & Cumming, USA). After curing at 70–80°C for 8 h, a ceramic fibre/epoxy 1-3 composite rod was formed. The volume fraction of

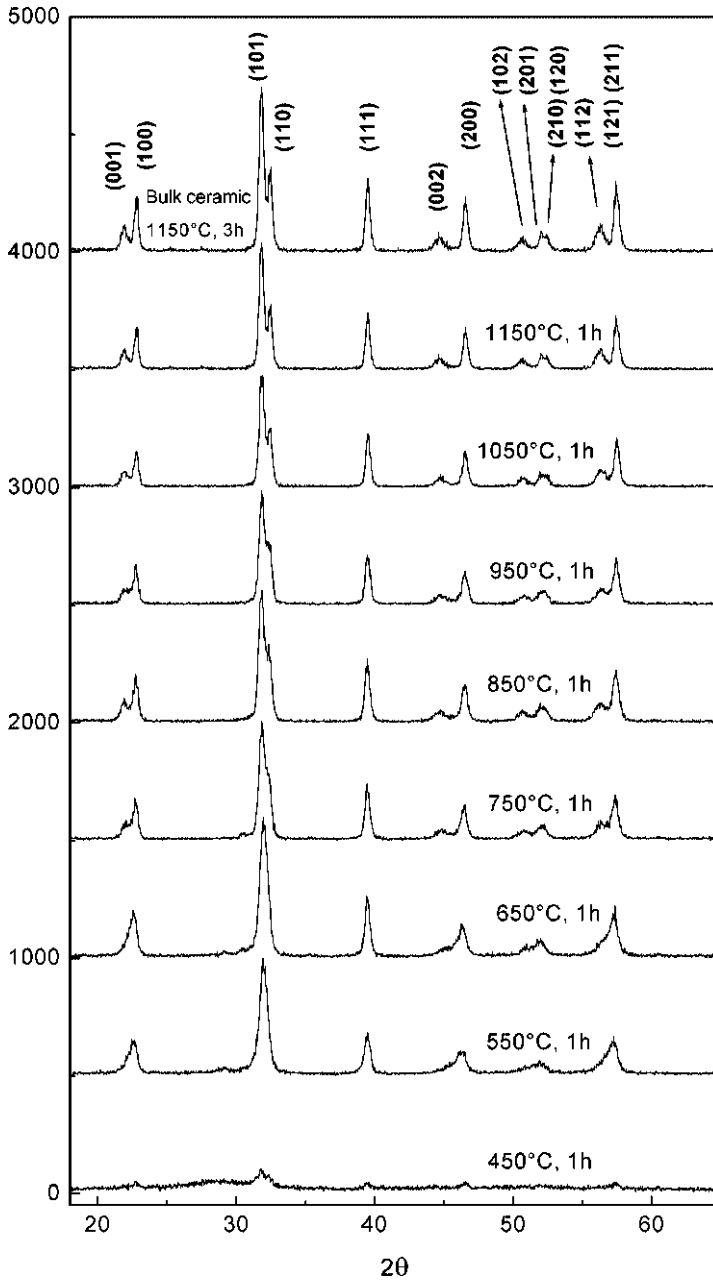


3.5 SEM micrographs of the PSmT ceramic fibres, which were fabricated by hydrolysing gel fibres at room temperature for two weeks and at 60–80°C in moist air for 48 h. The dried fibres were pyrolysed at 400°C for 1 h and at 550°C for 1 h before they were calcinated at 850°C for 2 h and then sintered at 1150°C for 1.5 h. (a) and (b) show the surface; and (c) and (d) the cross sections, of the PSmT ceramic fibre.¹⁹

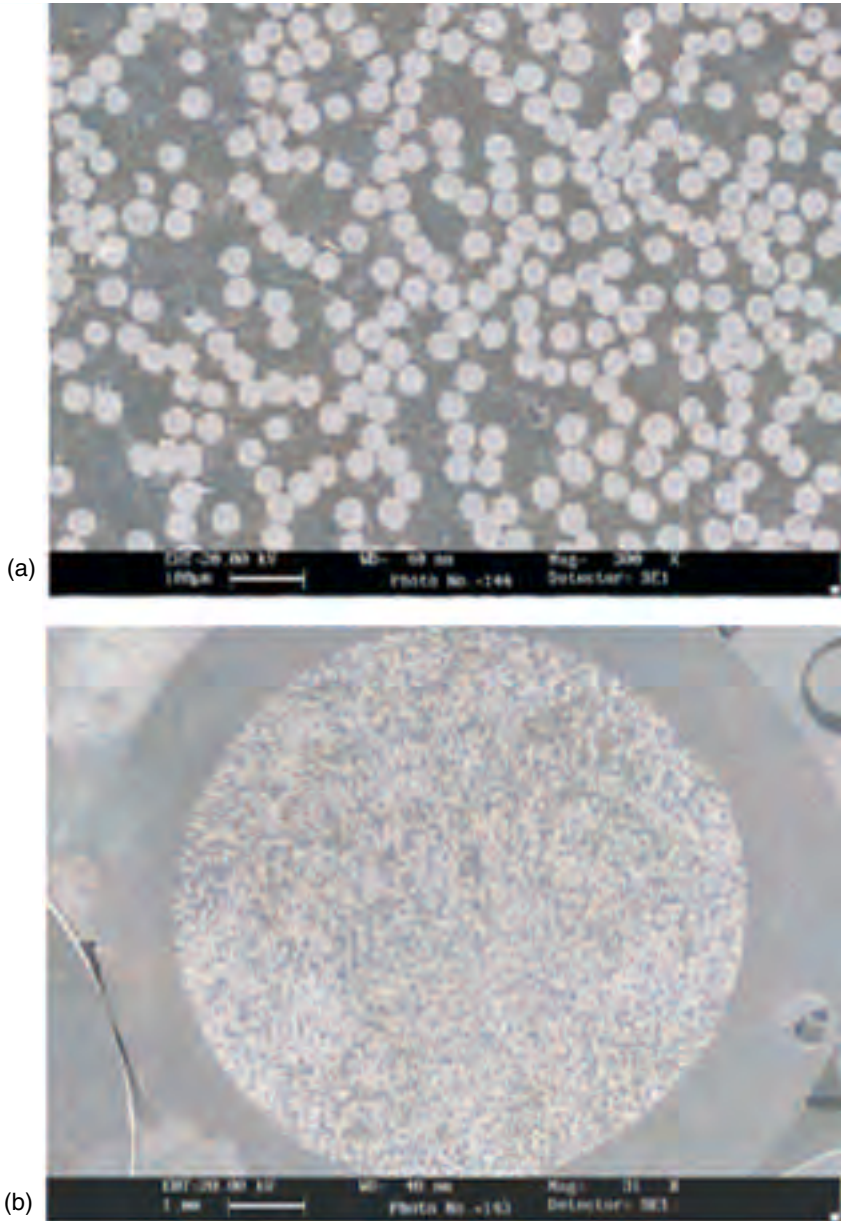
ceramics ϕ can be adjusted by changing the number of fibres inserted, and ϕ was calculated by the following equation:

$$\bar{\rho} = \phi\rho + (1 - \phi)\bar{\rho} \quad [3.1]$$

where $\bar{\rho}$, ρ and $\bar{\rho}$ are the density of the composite, ceramics and epoxy, respectively. The density of the samples was determined by applying the Archimedes principle. The composite rod was sliced into disks in the direction perpendicular to the rod axis. The composite disks were polished and chromium/gold electrodes were deposited on both sides of the disk. To elicit the piezoelectric properties in the fibres, they need to be polarised by applying an electric field to align the dipoles inside the ceramics. The poling was carried out at 110–120°C under an electric field of 4.5 kV mm⁻¹ for 15 min. The poled disks were short circuited for more than two days before they were measured using an HP4294A impedance/gain phase analyser and a d_{33} meter. Figure 3.7 shows the SEM micrograph of a PSmT fibre/epoxy 1-3 composite with a 0.4 volume fraction of PSmT. The ceramic fibres in this 1-3 composite have an average diameter of ~ 46 µm. To increase the ceramic



3.6 X-ray diffraction (XRD) patterns of the PSmT bulk ceramics and the PSmT ceramic fibres (crushed into powder before taking XRD patterns) heated at different temperatures.¹⁹



3.7 SEM micrographs of a PSmT ceramic fibre(46 μm)/epoxy 1-3 composite disk. The ceramic volume fraction is 0.4. (a) is an enlarged view of (b).¹⁹

volume fraction ϕ in the composite, it was necessary to tie the ceramic fibres tightly together using rubber tape on the outside of the plastic tube. The highest ϕ attained was 0.68. The volume fraction of ceramics ϕ can also be measured by integrating the area of the fibres under a scanning electron microscope. From the ratio of the area of the fibre and the epoxy, ϕ can be estimated.

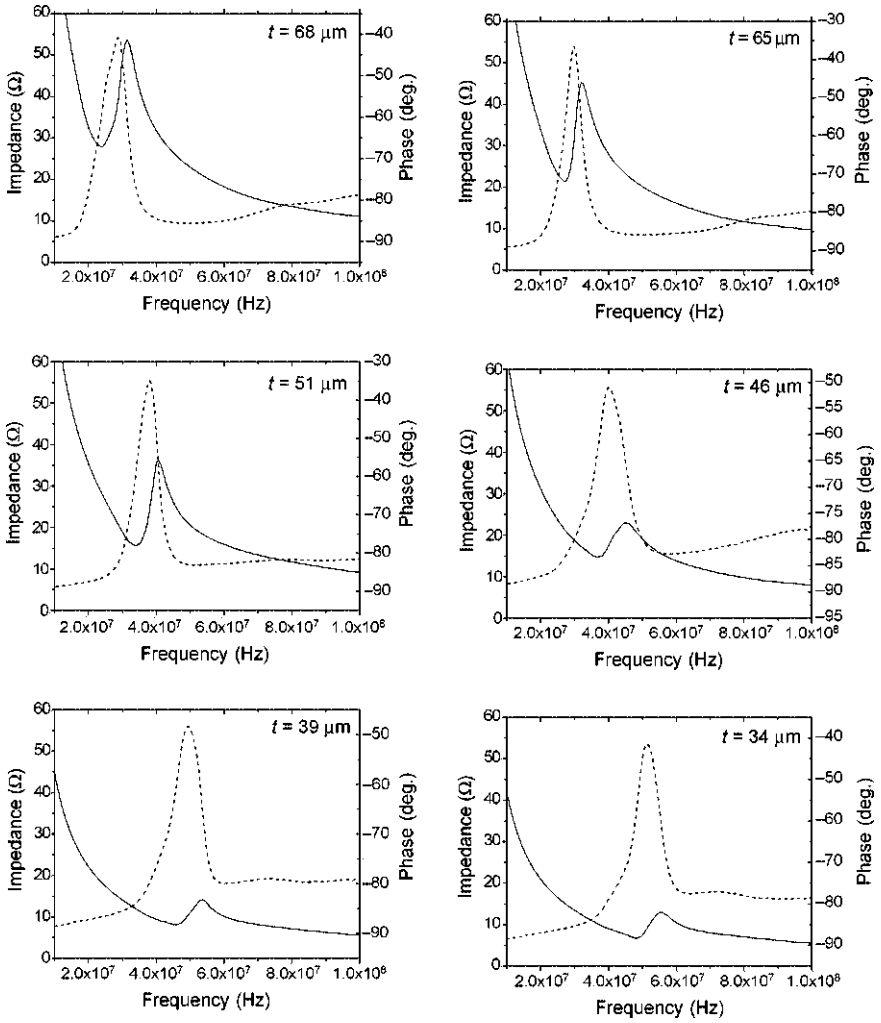
3.4 Electromechanical properties of ceramic fibre/epoxy 1-3 composites

Figure 3.8 shows the impedance and phase spectra of a PSmT fibre/epoxy 1-3 composite disk with a 4.5 mm diameter containing 35 μm diameter fibres in the frequency range of 10–100 MHz. The volume fraction of PSmT was 0.68. A strong thickness mode resonance was observed and other resonances were very weak. The thickness electromechanical coupling coefficient \bar{k}_t can be evaluated from data obtained from this resonance peak following IEEE standards.⁴⁷ It is noted that the impedance at the resonance frequency decreases as the thickness is reduced. In fact, the electrical impedance of the composite can be adjusted to be compatible with that of the driving electronics at the frequency of operation (e.g. adjust to 50 Ω). This is done by changing the ceramic volume fraction, thickness and surface area of the composite. The relative permittivity $\bar{\epsilon}_{33}^T$, piezoelectric \bar{d}_{33}^T coefficient, elastic compliance \bar{s}_{33}^E and \bar{k}_t of 1-3 composites with different volume fractions of PSmT fibres were measured. The experimental data are compared with the modelling results in the following section.

3.5 The modified parallel and series model of ceramic/polymer 1-3 composites

In order to use the composite materials in designated applications, it is important to be able to predict their performance. There are a number of proposed models^{27, 29–33, 36, 38–40, 45, 46} to evaluate the overall performance of ceramic/polymer 1-3 composites. Here, a modified parallel and series model^{29, 30, 36, 39} is described, as this simple model can give reasonable predictions of the materials parameters of 1-3 composites with $\phi > 0.1$. It can be used to calculate the material parameters of PSmT fibre/epoxy 1-3 composites. These figures can then be compared with the experimental data if we assume that the ceramic fibres have properties similar to those of the bulk PSmT ceramics. Alternatively, we can use the measured parameters of the composite and estimate the materials properties of the PSmT fibres by the model calculation.

In this analysis, the material parameters of epoxy are denoted by a double bar on the top of the parameters, while the effective material parameters of the composite are denoted by a bar. The following assumptions have been adopted in the model:^{30, 36}



3.8 The electrical impedance and phase spectra of PSmT fibre/epoxy 1-3 composites with different thickness t . The 4.5 mm diameter composite disk contains 35 μm diameter fibres and the ceramic volume fraction is 0.68.¹⁹

(1) The mechanical displacements are parallel to the coordinate axes, so that all shear components vanish in the x - y plane:

$$T_4 = T_5 = T_6 = \bar{T}_4 = \bar{T}_5 = \bar{T}_6 = 0 \quad [3.2]$$

$$S_4 = S_5 = S_6 = \bar{S}_4 = \bar{S}_5 = \bar{S}_6 = 0 \quad [3.3]$$

where T and S denote stress and strain, respectively.

(2) All fringing fields anywhere inside the materials are zero, giving:

$$E_1 = E_2 = \bar{E}_1 = \bar{E}_2 = 0 \quad [3.4]$$

$$D_1 = D_2 = \bar{D}_1 = \bar{D}_2 = 0 \quad [3.5]$$

where E and D are the electric field and electric displacement, respectively.

(3) The composite can be treated as an effective homogeneous medium; both the ceramics and epoxy move together in a uniform thickness oscillation and the vertical strains are the same in both phases (isostrain), giving:

$$\bar{S}_3 = S_3 = \bar{S}_3 \quad [3.6]$$

This leads to an effective total stress in the z direction, given by averaging over the contributions of the constituent phases:

$$\bar{T}_3 = \phi T_3 + (1 - \phi) \bar{T}_3 \quad [3.7]$$

(4) Electric fields are the same in both the ceramics and epoxy phases in the z direction:

$$\bar{E}_3 = E_3 = \bar{E}_3 \quad [3.8]$$

Thus, the effective total electric displacement is the average over the contributions of the two phases:

$$\bar{D}_3 = \phi D_3 + (1 - \phi) \bar{D}_3 \quad [3.9]$$

(5) The composite as a whole is laterally clamped, but not for the individual elements:

$$\bar{T}_1 = T_1 = \bar{T}_1 \quad [3.10]$$

$$\bar{T}_2 = T_2 = \bar{T}_2 \quad [3.11]$$

$$\bar{S}_1 = \phi S_1 + (1 - \phi) \bar{S}_1 \quad [3.12]$$

$$\bar{S}_2 = \phi S_2 + (1 - \phi) \bar{S}_2 \quad [3.13]$$

The 1-3 composites are considered as isotropic in the x - y plane so that all lateral components are equal $T_1 = T_2$, $\bar{T}_1 = \bar{T}_2$, $S_1 = S_2$, $\bar{S}_1 = \bar{S}_2$. Some important parameters of the composites, e.g. the relative permittivity $\bar{\epsilon}_{33}^T$, piezoelectric \bar{d}_{33}^T coefficient and compliance \bar{s}_{33}^E , can be derived^{19,30,36,39} as:

$$\bar{\epsilon}_{33}^T = \phi \epsilon_{33}^T + (1 - \phi) \bar{\epsilon}_{11}^T - \frac{\phi(1 - \phi)d_{33}^2}{S(\phi)} \quad [3.14]$$

$$\bar{d}_{33}^- = \frac{\phi d_{33}^- \bar{s}_{11}^-}{S(\phi)} \quad [3.15]$$

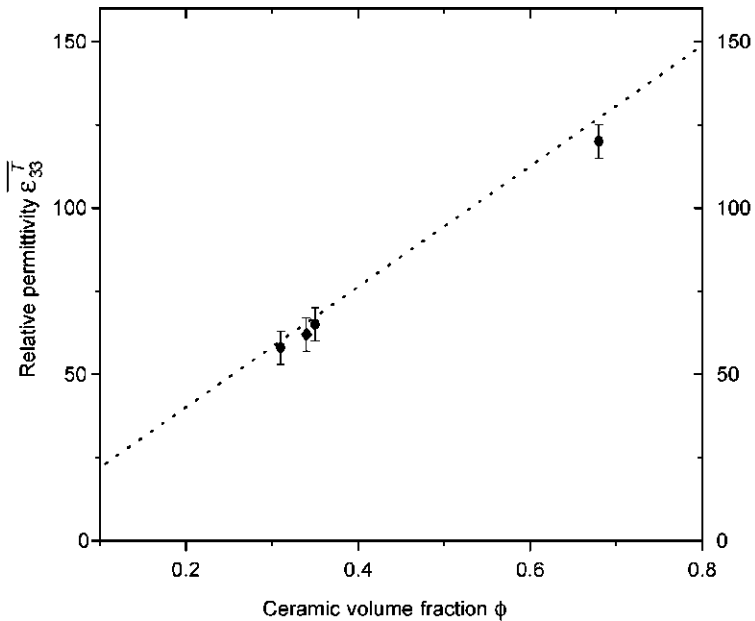
$$\bar{s}_{33}^E = \frac{s_{33}^E \bar{s}_{11}^-}{S(\phi)} \quad [3.16]$$

where

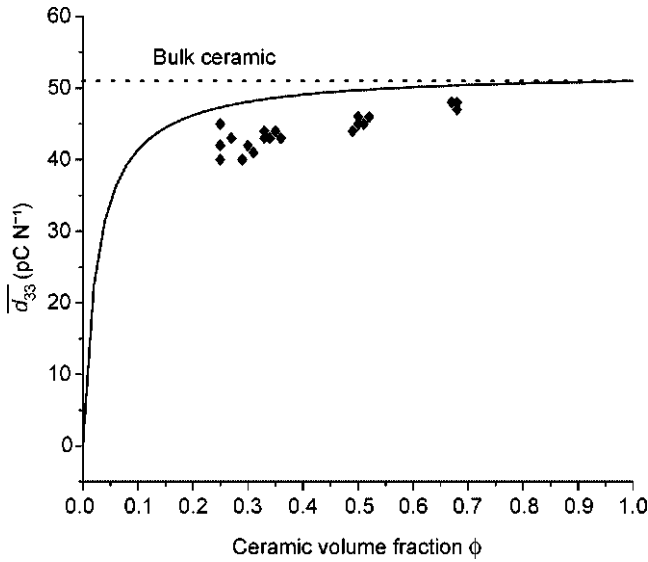
$$S(\phi) = \phi \bar{s}_{11}^- + (1 - \phi) s_{33}^E \quad [3.17]$$

where s_{33}^E is the elastic compliance of the ceramic fibre. Definitions of all of the symbols of piezoelectric ceramics can be found in the IEEE standards for piezoelectricity.⁴⁷

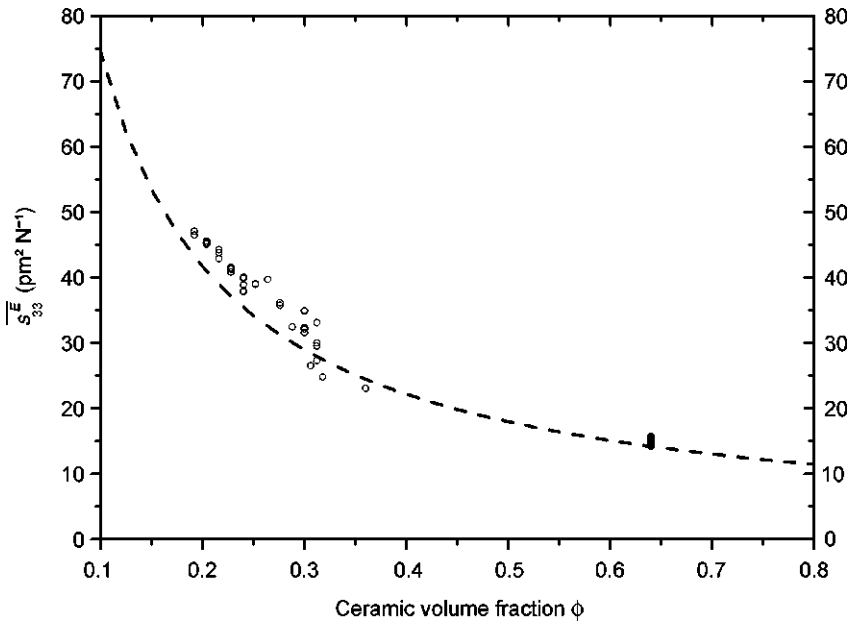
The measured values of $\bar{\epsilon}_{33}^T$, \bar{d}_{33}^- and \bar{s}_{33}^E of the PSmT 1-3 composites are plotted, together with the model calculations in Figs 3.9–3.11. Reasonable agreements are obtained showing that this simple model is useful in predicting the materials parameters of 1-3 composites. The measured electromechanical coupling coefficient \bar{k}_t of the composites is found to be higher than that of bulk ceramics, as shown in Fig. 3.12. This is because the ceramic fibres are actually not rigidly clamped by the soft polymer matrix and they can vibrate quite freely. Hence, \bar{k}_t of the composite is close to the k_{33} of a ceramic rod that has a higher value.^{30,36}



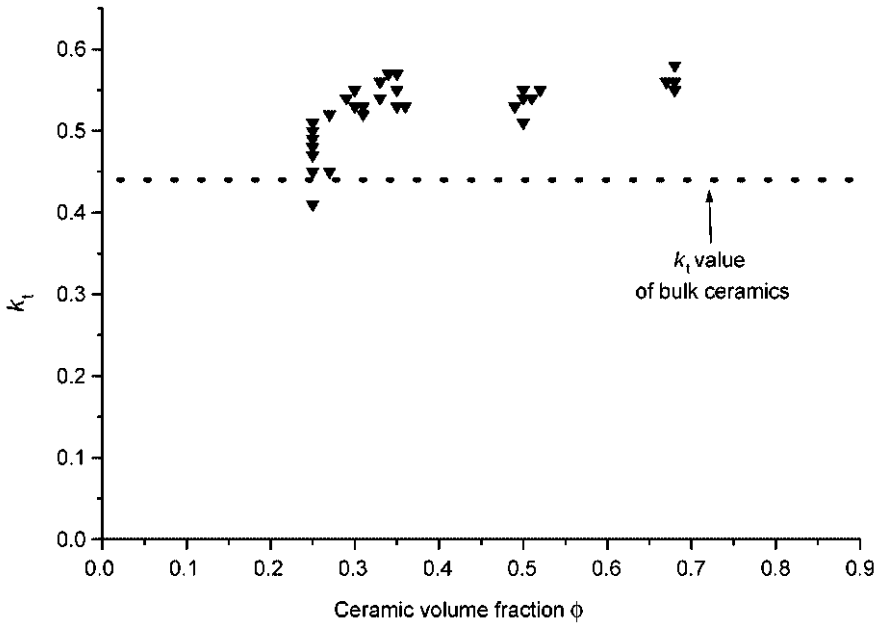
3.9 The relative permittivity $\bar{\epsilon}_{33}^T$ of the PSmT fibre/epoxy 1-3 composite as a function of ceramic volume fraction ϕ . The symbols and the line represent the experimental data and model calculation from Equation [3.14], respectively.¹⁹



3.10 The piezoelectric \overline{d}_{33} coefficient of the PSmT fibre/epoxy 1-3 composite as a function of ceramic volume fraction ϕ . The symbols and the solid line represent the experimental data and model calculation from Equation [3.15], respectively.¹⁹



3.11 The elastic compliance \overline{s}_{33}^E of the PSmT fibre/epoxy 1-3 composite as a function of ceramic volume fraction ϕ . The symbols and the line represent the experimental data and model calculation from Equation [3.16], respectively.¹⁹



3.12 The measured thickness electromechanical coupling coefficient \bar{k}_t of the PSmT fibre/epoxy 1-3 composite as a function of ceramic volume fraction ϕ . The line represents the k_t of the bulk PSmT ceramics.¹⁹

3.6 Possible uses of ceramic fibres and composites in intelligent apparel applications

The above discussions show, using PSmT ceramics as an example, the fabrication of ceramic fibres by a sol-gel process and the properties of 1-3 ceramic fibre/polymer composites. Different piezoelectric ceramics and polymers can be selected to optimise the composite performance for the designated applications. These ceramic fibre/polymer 1-3 composites are quite flexible and can be used as acoustic sensors to be incorporated into fabrics and clothing. They can be used to sense vibration, audible sound and ultrasound. They have adjustable density and acoustic impedance, which gives a better match with human tissue. Hence, these acoustic sensors can be used to optimise the transfer of acoustic energy from the human skin to the sensor. This is the distinct advantage of these composites compared to conventional ceramics. For example, they can be fabricated into acoustic sensors attached to a scarf or a belt and can be worn around the neck or wrist for health monitoring. These sensors can pick up heartbeats and breathing rates and, if equipped with wireless communication transmitter, can send the relevant information to a remote receiver. Different sizes of ceramic fibres can also be selected in the fabrication of composites. It is also possible to distribute the

fibres in groups to form necessary array patterns. These acoustic arrays can be used to detect sound, and monitor and locate the source of the sound. As 1-3 composites have higher d_{33} coefficients compared with piezoelectric polymer vinylidene fluoride–trifluoroethylene [P(VDF-TrFE)]. They can replace P(VDF-TrFE) copolymer in a number of applications, for example, as actuators and for recovering some of the power in the process of walking in piezoelectric shoe inserts.^{48–50} Although 1-3 composites have been widely used in medical ultrasound and underwater acoustics, their use in intelligent apparel and wearable electronics has just begun and more innovative applications can be envisaged in the future.

3.7 Acknowledgements

The support provided by the Hong Kong Research Grants Council and the Centre for Smart Materials of The Hong Kong Polytechnic University is gratefully acknowledged.

3.8 References

- Berlincourt DA, Curran DR and Jaffe H, 'Piezoelectric and piezomagnetic materials and their function in transducers', *Physical Acoustics*, Vol. 1, Part A, New York, Academic Press, 1964, 169–270.
- Jaffe B, Cook WR Jr and Jaffe H, 'The piezoelectric effect in ceramics', in J P Roberts and P Popper (eds), *Piezoelectric Ceramics*, London and New York, Academic Press, 1971, 7–23.
- Mitsui T, Tatsuzaki I and Nakamura E, *An Introduction to the Physics of Ferroelectrics*, London, Gordon and Breach Science, 1976, 1–7.
- Ikeda T, *Fundamentals of Piezoelectricity*, Tokyo, Oxford University Press, 1990, 119–121.
- Xu Y H, *Perovskite-type Ferroelectrics: Part I, Ferroelectrics materials and their applications*, Amsterdam and New York, Elsevier Science, 1991, 101–162.
- Yoshikawa S, Selvaraj U, Brooks K and Kurtz S, 'Piezoelectric PZT tubes and fibers for passive vibration damping', *Proceedings 8th IEEE International Symposium on Applications of Ferroelectrics*, USA, IEEE, 1992, 269–272.
- Janas V F and Ting S M, 'Fine-scale, large area piezoelectric fiber/polymer composites for transducer applications', *Proceedings 9th IEEE International Symposium on Applications of Ferroelectrics*, USA, IEEE, 1994, 1, 295–298.
- Meyer R J, *Fabrication of Perovskite Lead Zirconate Titanate and Barium Strontium Titanate Fibers using Sol–Gel Technology*, MSc Thesis, The Pennsylvania State University, USA, 1995.
- Meyer R J, Shrout T R and Yoshikawa S, 'Development of ultra-fine scale piezoelectric fibres for use in high frequency 1-3 transducers', *Proceedings 10th IEEE International Symposium on Application of Ferroelectrics*, Switzerland, IEEE, 1996, 2, 547–550.
- Jadidian B, Janas V and Safari A, 'Development of fine scale piezoelectric ceramic/polymer composites via incorporation of fine PZT fibers', *Proceedings 10th IEEE International Symposium on Application of Ferroelectrics*, Switzerland, IEEE, 1996, 1, 31–34.

11. Meyer R J, *High Frequency (15–70 MHz) 1-3 PZT Fiber/Polymer Composites: Fabrication and Characterization*, PhD Thesis, The Pennsylvania State University, USA, 1998.
12. Glaubitt W, Sporn D and Rainer J, 'Sol-gel processing of functional and structural ceramic oxide fibers', *J. Sol-Gel Sci. Technol.*, 1997, **8**, 29–33.
13. Sporn D, Watzka W, Pannkoke K and Schonecker A, 'Smart structures by integrated piezoelectric thin fibers(I): preparation, properties and integration of fibers in the System $\text{Pb}(\text{Zr},\text{Ti})\text{O}_3$ ', *Ferroelectrics*, 1999, **224**, 1–6.
14. Schonecker A, Keitel U, Kreher W, Sporn D, Watzka W and Pannkoke K, 'Smart structures by integrated piezoelectric thin fibers (II): properties of composites and their physical description', *Ferroelectrics*, 1999, **224**, 7–12.
15. Sporn D, Watzka W, Schonecker A and Pannkoke K, 'Smart structure by integrated piezoelectric thin fibers', in *Piezoelectric Materials: Advances in Science, Technology and Applications*, C Galassi (ed), Netherlands, Kluwer Academic, 2000, 87–97.
16. Steinhausen R, Hauke T, Beige H, Watzka W, Lange U, Sporn D, Gebhardt S and Schonecker A, 'Properties of fine scale piezoelectric PZT fibers with different Zr content', *J. Eur. Ceram. Soc.*, 2001, **21**, 1459–1462.
17. Steinhausen R, Hauke T, Seifert W, Beige H, Watzka W, Seifert S, Sporn D, Starke S and Schonecker A, 'Finescaled piezoelectric 1-3 composites: properties and modeling', *J. Eur. Ceram. Soc.*, 1999, **19**, 1289–1293.
18. Watzka W and Seifert S, 'Dielectric and ferroelectric properties of 1-3 composites containing thin PZT-fibers', *Proceedings 10th IEEE International Symposium on Application of Ferroelectrics*, Switzerland, IEEE, 1996, **2**, 569–572.
19. Li K, *Piezoelectric Ceramic Fibre/Polymer 1-3 Composites for Transducer Applications*, PhD Thesis, The Hong Kong Polytechnic University, 2002.
20. Li K, Wang D Y, Lam K H, Chan H L W and Choy C L, 'Samarium and manganese doped lead titanate ceramic fiber/epoxy 1-3 composites for high frequency transducer applications', *Proceeding of PRICM4 2001*, USA, Japan Institute of Metals, 2001, **2**, 1603–1606.
21. Li K, Lam K H, Wang D Y, Chan H L W and Choy C L, 'Preparation of Li, Nb and Mn doped PZT ceramic fibers and ceramic fiber/epoxy 1-3 composites', *Proceeding of PRICM4 2001*, USA, Japan Institute of Metals, 2001, **2**, 1583–1586.
22. Li K, Chan H L W and Choy C L, 'Samarium and manganese doped lead titanate ceramic fiber/epoxy 1-3 composites for high frequency transducer applications', *IEEE Trans. on Ultrasonics, Ferroelectrics and Frequency Control*, 2003, **50**(10), 1371–1376.
23. Li K, Chan H L W and Choy C L, 'Study of zinc and niobium modified lead zirconate titanate fiber/epoxy 1-3 composites', *Jpn. J. Appl. Phys.*, 2002, **41**, 6989–6992.
24. Chan H L W, Li K and Choy C L, 'Piezoelectric ceramic fiber/epoxy 1-3 composites for high-frequency ultrasonic transducer applications', *Mat. Sci. Eng., B*, 2003, **99**, 29–35.
25. Newnham R E, Skinner D P and Cross L E, 'Connectivity and piezoelectric composites', *Mater. Res. Bull.*, 1978, **13**, 525–536.
26. Klicker K A, Bigger J V and Newnham R E, 'Composites of PZT and epoxy for hydrostatic transducer applications', *J. Am. Ceram. Soc.*, 1981, **64**, 5–8.
27. Gururaja T R, Schulze W A, Cross L E, Newnham R E, Auld B A and Wang Y J, 'Piezoelectric composite materials for ultrasonic transducer applications', *IEEE Trans. Sonics and Ultrasonics*, 1985, **SU-32**(4), 481–498.
28. Gururaja T R, Schulze W A, Cross L E and Newnham R E, 'Piezoelectric composite materials for ultrasonic transducer applications. Part II: Evaluation of ultrasonic medical applications', *IEEE Trans. Sonics and Ultrasonics*, 1985, **SU-32**(4), 499–523.

29. Chan HL W, *Piezoelectric Ceramic/Polymer 1-3 Composites for Ultrasonic Transducer Applications*, PhD Thesis, Macquarie University, Australia, 1987.
30. Chan H L W and Unsworth J, 'Simple model for piezoelectric ceramic/polymer 1-3 composites used in ultrasonic transducer applications', *IEEE Trans. Ultrasonics, Ferroelectrics and Frequency Control*, 1989, **36**(4), 434–441.
31. Hayward G and Hossack J A, 'Unidimensional modeling of 1-3 composite transducers'. *J. Acoust. Soc. Am.*, 1990, **88**(2), 599–608.
32. Smith W A, 'Modeling 1-3 composite piezoelectrics: thickness-mode oscillations', *IEEE Trans. on Ultrasonics, Ferroelectrics and Frequency Control*, 1991, **38**, 40–47.
33. Hossack J A and Hayward G, 'Finite element analysis of 1-3 composite transducers', *IEEE Trans. Ultrasonics, Ferroelectric and Frequency Control*, 1991, **38**(6), 618–629.
34. Slayton M H and Setty H S N, 'Single layer piezoelectric-epoxy composite', *Proceedings IEEE Ultrasonics Symposium*, 1991, 90–92.
35. Waller D J, Safari A and Card R J, 'Woven PZT ceramic/polymer composites for transducer application', *Proceedings 7th IEEE International Symposium on Application of Ferroelectrics*, 1991, 82–85.
36. Smith W A, 'Modeling 1-3 composite piezoelectrics: hydrostatic response', *IEEE Trans. on Ultrasonics, Ferroelectrics and Frequency Control*, 1993, **40**(1), 41–49.
37. Brown L J, Gentilman R L, Pham H T, Fiore D F and French K W, 'Injection molded fine-scale piezoelectric composite transducers', *Proceedings IEEE Ultrasonics Symposium*, 1993, **1**, 499–503.
38. Taunamang H, Guy I L and Chan H L W, 'Electromechanical properties of 1-3 piezoelectric ceramic/piezoelectric polymer composites', *J. Appl. Phys.*, 1994, **76**(1), 484–489.
39. Chan HL W and Guy IL, 'Piezoelectric ceramic/polymer composites for high frequency applications', *Key Eng. Mat.*, 1994, **92–93**, 275–300.
40. Nowicki A, Kycia K, Iien T D, Gaji O and Klciber M, 'Numerical calculations of the acoustic properties of the 1-3 composite transducers for medical applications', *IEEE Ultrasonics Symposium*, 1995, 1041–1044.
41. Janas V F and Safari A, 'Overview of fine-scale piezoelectric ceramic/polymer composite processing', *J. Am. Ceram. Soc.*, 1995, **78**(11), 2945–2955.
42. Pazol B G, Bowen L J, Gentilman R L, Pham H T and Serwatka W J, 'Ultrafine scale piezoelectric composite materials for high frequency ultrasonic imaging arrays', *IEEE Ultrasonic Symposium*, 1995, 1263–1268.
43. Panda R K, Janas V F and Safari A, 'Fabrication and properties of fine 1,3-composites by modified lost mold method', *Proceedings 10th IEEE International Symposium on Application of Ferroelectrics*, 1996, **2**, 551–554.
44. Hayward G and Bennett J, 'Assessing the influence of pillar aspect ratio on the behavior of 1-3 connectivity composite transducers', *IEEE Trans. on Ultrasonics, Ferroelectrics and Frequency Control*, 1996, **43**(1), 98–108.
45. Takeuchi Y, Nozaki R, Hirata Y, Takada H and Smith L S, 'Novel 1-3 piezo-composites using synchrotron radiation lithography and its application for high frequency medical arrays', *Proceedings IEEE Ultrasonics Symposium*, 1997, **2**, 919–922.
46. Certon D, Casula O, Patat F and Royer D, 'Theoretical and experimental investigations of lateral modes in 1-3 piezocomposites', *IEEE Trans. on Ultrasonics, Ferroelectrics and Frequency Control*, 1997, **44**(3), 643–651.
47. IEEE Standard on Piezoelectricity, ANSI/IEEE Std 176, 1987, 227–273.

48. Starner T, 'Human-powered wearing computing', *IBM System J.*, 1996, **35**(3/4), 618–629.
49. Smalser, *Power Transfer of Piezoelectric Generated Energy*, US Patent Office, Pat No 5 703 474, 1997.
50. Lacic N, *Inflatable Boot Liner with Electrical Generator and Heater*, US Patent Office, Pat No 4 845 338, 1989.